NASA CONTRACTOR REPORT

NASA CR-2578

NASA CR-2578

TRANSONIC AIRFOIL DESIGN USING CARTESIAN COORDINATES

Leland A. Carlson

Prepared by
TEXAS A&M RESEARCH FOUNDATION
College Station, Tex. 77840
for Langley Research Center

NATIONAL AERONAUTICS AND SPACE ADMINISTRATION • WASHINGTON, D. C. • APRIL 1976

1. Report No.	2. Government Accession No.	3. Recipient's Catalog No.
CR-2578		

4. Title and Subtitle	5. Report Date
TRANSONIC AIRFOIL DESIGN USING CARTESIAN COORDINATES	April 1976
	6. Performing Organization Code

7. Author(s)	8. Performing Organization Report No.
Leland A. Carlson	

9. Performing Organization Name and Address	10. Work Unit No.
Texas A&M Research Foundation College Station, TX 77840	501-06-05-08-00
	11. Contract or Grant No.
	NGR-44-001-157

12. Sponsoring Agency Name and Address	13. Type of Report and Period Covered
National Aeronautics and Space Administration Washington, D.C. 20546	CONTRACTOR REPORT
	14. Sponsoring Agency Code

15. Supplementary Notes

Monitored by Jerry C. South, Jr., Mail Stop 360
Langley Research Center, Hampton, VA 23665

Final Report

16. Abstract

A numerical technique for designing transonic airfoils having a prescribed pressure distribution (the inverse problem) is presented. The method employs the basic features of Jameson's iterative solution for the full potential equation, except that inverse boundary conditions and Cartesian coordinates are used. The method is a direct-inverse approach that controls trailing-edge closure. Examples show the application of the method to design aft-cambered and other airfoils specifically for transonic flight.

17. Key Words (Suggested by Author(s))	18. Distribution Statement
Supercritical airfoil design Relaxation Cartesian coordinates Inverse problem	Unclassified - Unlimited Subject Category 02

19. Security Classif. (of this report)	20. Security Classif. (of this page)	21. No. of Pages	22. Price*
Unclassified	Unclassified	33	$3.75

*For sale by the National Technical Information Service, Springfield, Virginia 22161

TRANSONIC AIRFOIL DESIGN USING CARTESIAN COORDINATES

By Leland A. Carlson
Texas A&M University

SUMMARY

A numerical technique for designing transonic airfoils having a prescribed pressure distribution (the inverse problem) is presented. The method employs the basic features of Jameson's iterative solution for the potential equation, except that inverse boundary conditions and Cartesian coordinates are used. The method utilizes a direct-inverse approach that leads to a logical method for controlling trailing edge closure. Examples show the application of the method to design aft-cambered and other airfoils specifically for transonic flight.

INTRODUCTION

A numerical method for the design of transonic airfoils should not only be accurate but also be as simple as possible in concept and approach. It should use coordinate systems, input variables, and boundary condition treatments that can be easily understood by the user. In addition, it would be desirable if the method yielded the airfoil design shape for a given set of conditions with little or no iteration and used or computed nose and tail shapes that are aerodynamically and structurally reasonable. Finally, it should be able to handle both shocked and shockless flows and be suitable for not only complete design but also airfoil modification.

Previous design methods and programs have either worked with the hodograph equations,[1,2] used direct[3] optimization techniques, or tried the inverse approach.[4-7] Of these, probably the best known are the hodograph methods of Nieuwland[1] and of Bauer, Garabedian, and Korn.[2] While these methods yield excellent accurate results, they are restricted to shock free solutions which may have adverse drag, pitching moment, and boundary layer separation characteristics at off-design conditions.[8] Further, they are difficult from the user standpoint in that they involve complex mappings and transformations and require complicated initial input conditions. In Nieuwland's method, the user

must a priori specify the trailing edge Mach number and flow angle, while in the Korn theory a set of logarithmic terms must be given involving singularities inside the airfoil. As a consequence the hodograph methods may require a large number of trial solutions before an acceptable airfoil design is achieved,[7] and they are not suitable for simple airfoil modification since there seems to be no straight forward way of changing only part of the solution.

Another design technique is to use a direct method (airfoil prescribed) to analyze the flow about a given airfoil and then, based upon this result, to modify the airfoil in an attempt to satisfy the design conditions. Usually this approach requires extensive experience on the part of the user and a large number of iterations. It can, however, yield good results. Recently, Hicks, Murman, and Vanderplaats[3] have automated this procedure for non-lifting airfoils by combining a transonic, small perturbation analysis program with an optimization program based on the method of feasible directions. While very promising, the method tends to yield airfoils having multiple upper surface supersonic zones, which at off-design conditions may lead to multiple shocks and other adverse effects. In addition, it needs to be extended to lifting airfoils before its full usefulness can be ascertained.

The last design formulation is the inverse method in which the airfoil surface pressures or velocities are specified and the airfoil shape subsequently determined. Admittedly this approach requires knowledge of what would be a desirable pressure distribution, but this characteristic is probably understood by the designer as well as, if not better than, any other. Furthermore, the designer can a priori select a pressure distribution that will yield a given lift and moment, have a reasonable supersonic zone, behave desirably with respect to boundary layer separation, and satisfy other transonic flow criteria. Of course, the resultant airfoil design shape may or may not be physically and structurally reasonable.

The inverse approach was initially pursued by Erdos, Baronti, and Elzweig[4] and by Steger and Klineberg.[5] Both groups used the transonic small perturbation equations and formulated the problem in a direct-inverse manner. That is, the leading edge shape was specified and that region solved directly, while on the remainder of the airfoil the pressure was prescribed and the shape

computed. Erdos et al used the perturbation potential as the basic unknown everywhere in the flowfield, but Steger and Klineberg used the perturbation potential only in the direct region. In the inverse zone, they posed the problem in terms of the perturbation velocities. Since each approach solved the flow directly up to an arbitrary point, each could be used, if desired, to analyze a problem in a completely direct mode. Now if the pressure distribution from such a direct computation were used as input for an inverse calculation, the original airfoil shape should be recovered. Yet, Erdos et al obtained in that case a discontinuity in body slope at the location of the shock wave, which they attributed to the singular nature of the point of intersection between the shock and the surface boundary. Steger and Klineberg experienced similar phenomena but determined that they were numerical in origin and that they could be eliminated with careful formulation. Unfortunately, since the two methods used different dependent variables in the inverse zone, the self-consistency of an approach using only the perturbation potential was not established.

This problem was subsequently investigated in detail[6] and it was established that the discontinuity observed by Erdos was strictly numerical in origin and that inverse results consistent with direct calculations could be obtained using the perturbation potential. In addition, it was demonstrated by using experimentally measured pressures as input that inverse transonic calculations are capable of reflecting the consequences of viscous-inviscid interaction on the airfoil displacement surface shape. Finally, it was determined that the inverse approach using the small perturbation equations tended to become inaccurate for thick and blunt-nosed airfoils.

Quite obviously the latter problem can be eliminated by formulating the inverse problem with the complete potential flow equation. Unfortunately, this makes the problem more difficult in that unlike the small disturbance case the location of the airfoil surface boundary condition in the computational plane is unknown. Tranen[7] applied the complete equations to the inverse problem by modifying the conformal mapping relaxation solution technique of Garabedian and Korn to use the pressure distribution boundary condition. Since this technique maps the computational grid to match the airfoil surface, Tranen was forced to apply the boundary conditions at the surface of some assumed airfoil.

Only after the relaxation process had converged could a new shape be computed; and, usually, because of the difference between where the boundary conditions were and should have been applied, the resultant shape was not completely compatible with the input pressure distribution. Tranen solved this problem by resorting to, for each case, a series of inverse-direct-inverse-direct, etc. calculations in which the pressure distribution was modified prior to each inverse calculation. This was done in an attempt to achieve convergence, which occurred when the C_p distribution from a direct computation agreed with that used as input in the previous inverse run.

Tranen's work is significant because it successfully applies the complete equations to the inverse design problem and because it designs the entire airfoil. Since the method is entirely inverse and since in the inverse region the surface boundary condition specifies the derivative of ϕ in the streamline direction, an initial value of ϕ at the nose must be assumed. Unfortunately, the solution is sensitive to this value. Furthermore, to achieve convergence, Tranen's approach requires large scale iteration involving an unspecified modification of the input pressure distribution.

The purpose of this report is to present and discuss a new numerical method suitable for the design and/or modification of subsonic and transonic airfoils. In order to achieve accuracy, the method utilizes the full inviscid potential flow equations; and in order to remain simple, it solves the problem in a stretched Cartesian grid system. The resultant working computer program has several unique features. First, it can be used in either the direct (analysis) mode in which the airfoil shape is prescribed and the flowfield and surface pressures are determined, or in the direct-inverse (design) mode in which an initial nose shape is given along with the pressure distribution on the remainder of the airfoil and the flowfield and actual airfoil shape are computed. Second, it uses for the first time in a design program the rotated difference scheme introduced by South and Jameson,[10,11] which always has the correct zone of dependence in supersonic zones but does not require the coordinate system to be closely aligned to the flow direction. Third, unlike previous methods, the present program determines the airfoil shape simultaneously with the flowfield relaxation solution. Thus, when the converged solution is achieved, an airfoil design compatible with the input pressure distribution is known,

and iteration is not required.

This report primarily discusses the design mode of the program, presents the numerical features peculiar to the design problem, and shows how the method can be applied. A discussion of the analysis aspects of the method along with the numerical methods utilized, finite difference formulation, and numerical stability are presented in Reference 12.

SYMBOLS

a	isentropic speed of sound
a,b	coordinate stretching constants
c	chord length
C_p	pressure coefficient, $(p-p_\infty)/(\frac{1}{2}\rho_\infty U_\infty^2)$
C_L	lift coefficient
C_{MLE}	coefficient of moment about the leading edge
f,g	coordinate stretching functions
M	Mach number
p	pressure
q	velocity
U,V	velocity component in the x-, y- direction respectively
x,y	Cartesian coordinates
α	angle of attack
γ	ratio of specific heats
Γ	circulation
θ	polar coordinate
ξ,η	computational coordinates
ρ	density
Φ	potential function, Eq. (1)
ϕ	perturbation potential, Eq. (2)

Subscripts:

∞	freestream condition
b	body
TE	trailing edge
i,j	grid location
ξ,η,x,y	differentiation, i.e., $f_x = \frac{\partial f}{\partial x}$

PROBLEM FORMULATION

The exact equation for the potential function for two dimensional compressible flow can be written in Cartesian coordinates as

$$(a^2 - \Phi_x^2)\Phi_{xx} - 2\Phi_x\Phi_y\Phi_{xy} + (a^2 - \Phi_y^2)\Phi_{yy} = 0 \tag{1}$$

where the subscripts denote partial differentiation. By defining a perturbation potential, ϕ, such that

$$\Phi = xq_\infty\cos\alpha + yq_\infty\sin\alpha + q_\infty\phi \tag{2}$$

where the velocity components are given by,

$$U = \Phi_x = q_\infty(\cos\alpha + \phi_x) \tag{3a}$$

$$V = \Phi_y = q_\infty(\sin\alpha + \phi_y) \tag{3b}$$

the governing equation for the perturbation potential becomes

$$(a^2 - U^2)\phi_{xx} - 2UV\phi_{xy} + (a^2 - V^2)\phi_{yy} = 0 \tag{4}$$

with

$$a^2 = a_\infty^2 - \frac{\gamma-1}{2}[U^2 + V^2 - q_\infty^2] \tag{5}$$

The appropriate boundary condition at infinity is[13]

$$\phi = \frac{-\Gamma}{2\pi}\,\mathrm{Tan}^{-1}\left(\sqrt{1-M_\infty^2}\,\mathrm{Tan}(\theta - \alpha)\right) \tag{6}$$

where θ is the polar angle, and Γ is the circulation, which is determined by the change in potential across the Kutta-Joukowski cut at the trailing edge of the airfoil, i.e.

$$\Gamma = (\phi_{y=0^+} - \phi_{y=0^-})_{\text{Trailing Edge}} \tag{7}$$

As mentioned in the Introduction, in the design mode the shape of the nose region (typically 6-10% of the chord) is specified and the pressure is prescribed over the remainder of the airfoil. This procedure is used for several reasons. First, the nose region must be very accurately known in order to correctly fabricate an airfoil. Thus, by prescribing the nose shape, a possible major source of error is eliminated from the design procedure. Second, the boundary condition in the inverse region specifies the derivative of the perturbation potential in the tangential direction, and a starting value

must be known. With the present scheme, this value is determined by the direct solution in the nose region and need not be estimated or iterated for. Third, in some cases the designer may wish only to modify the aft portion of the airfoil. This can be done with the present scheme since the switch point from direct to inverse can be set by an input variable anywhere from about 6% chord to the trailing edge. Finally, and perhaps most importantly, specification of the nose shape gives the designer a physical entity whereby he can control the degree of closure of the trailing edge. This feature will be discussed later.

With this philosophy, the appropriate airfoil boundary condition in the direct region near the leading edge is

$$\left(\frac{dy}{dx}\right)_b = \left(\frac{V}{U}\right)_b = \frac{q_\infty(\cos\alpha+\phi_{x_b})}{q_\infty(\sin\alpha+\phi_{y_b})} \tag{8}$$

In the inverse region where the pressure is specified, the pressure coefficient expression can be solved for either ϕ_x or ϕ_y, since the tangential derivative involves both. If the inverse region included the leading edge region, the logical choice would be to use ϕ_y near the nose, since the flow there is primarily in the y direction, and ϕ_x downstream. However, since in the present problem the nose is not normally part of the inverse region, the appropriate inverse boundary condition is

$$(\phi_x)_b = -\cos\alpha + \left\{\frac{1}{1+\left(\frac{V^2}{U^2}\right)_b}\left\{1 - \left\{\left[1 + \frac{\gamma M_\infty{}^2 C_{p_b}}{2}\right]^{\frac{\gamma-1}{\gamma}} - 1\right\}\frac{2}{(\gamma-1)M_\infty{}^2}\right\}\right\}^{1/2} \tag{9}$$

Equation (9) is nonlinear in that ϕ_x, $U_b{}^2$, and $V_b{}^2$ all involve values of ϕ at various grid points. The treatment of this nonlinearity will be discussed in the next section.

Equation (8) is applied on the assumed nose shape, and in the inverse region Equation (9) is applied at the location of the current airfoil surfaces. The latter are determined by integration of the Equation (8) in the inverse region.

To facilitate the application of the infinity boundary condition, Equation (6), the coordinate stretching represented on Figure 1 was selected. Here

the x-y plane is the physical plane and ξ-η represents the computational plane, and each is subdivided into three regions. The stretching is symmetrical about the origin and is given by

$$x = x_4 + A_2 \mathrm{Tan}[\tfrac{\pi}{2}(\xi - \xi_4)] + A_3 \mathrm{Tan}[\tfrac{\pi}{2}(\xi - \xi_4)^3] \tag{10}$$

in region III and by

$$x = \xi(a + b\xi^2) \tag{11}$$

in region II. The constants a and b are determined by the requirements

$$x = x_4 \quad \text{at} \quad \xi = \xi_4 \tag{12a}$$

and

$$\frac{dx}{d\xi} = \frac{\pi A_2}{2} \quad \text{at} \quad \xi = \xi_4 \tag{12b}$$

The constant A_2 controls the grid spacing in the vicinity of X_4, which is usually near the leading and trailing edges; while A_3 determines the physical location of the grid adjacent to the grid edge.

In the y-direction the stretching relationship is given by

$$y = A_1 \mathrm{Tan}(\tfrac{\pi}{2}\eta) \tag{13}$$

where A_1 controls the grid size near the airfoil. Here, only a one parameter stretching is used in order to facilitate the transformation from computational to the physical ordinates, which is required each time the unknown airfoil surface is computed from Equation (8).

Notice that these stretchings map the infinite x,y plane

$$\begin{aligned} -\infty \leq x \leq \infty \\ -\infty \leq y \leq \infty \end{aligned} \tag{14}$$

into the finite computational plane

$$\begin{aligned} -(1 + \xi_4) \leq \xi \leq (1 + \xi_4) \\ -1 \leq \eta \leq 1 \end{aligned} \tag{15}$$

where ξ_4 determines the amount of the computational plane confined to the vicinity of the airfoil.

The governing equations formulated in terms of the ξ-η variables are then written in finite difference form and solved iteratively using numerical

relaxation. The finite differences are formulated using a rotated scheme, first proposed by South and Jameson,[10,11] which always has the correct zone of dependence in supersonic regions but does not require the coordinate system to be closely aligned to the flow direction. Essentially, the finite difference expressions are arranged to exhibit the basic features of a local rotation to the streamline direction.

With respect to the rotated difference scheme, it should be noted that the present approach is somewhat different from that used in Ref. (10) and (11). While still using rotation and viewing the relaxation process as a time-like procedure, time terms in the streamwise direction are not introduced implicitly as a consequence of the manner in which the difference expressions are formulated. Instead they are added explicitly and, as in Ref. (10) and (11), used as damping terms to control the stability and convergence of the relaxation process. By explicitly adding these time-like terms, no additional damping is required. Further, the amount of damping required can be easily determined by the user from the maximum local Mach number, which in the design problem would be known from the assumed surface pressure distribution. Also notice that the time-like terms correspond to the change in ϕ between relaxation cycles; and, thus, they approach zero as the solution converges. A detailed discussion of the finite difference formulation, the numerical scheme, and its stability is presented in Reference (12).

SURFACE BOUNDARY CONDITIONS AND COMPUTATION OF SHAPE

There are many ways to approximate the flow tangency, Equation (8), or surface pressure, Eq. (9), condition at the airfoil boundary. One approach, which is used here, is to generate dummy values of ϕ at mesh points inside the boundary such that the usual difference equations can be solved at all points outside the boundary. The problem is to develop a scheme for providing and updating these dummy values by using the surface tangency or pressure condition and neighboring values of ϕ in the mesh, with adequate accuracy and without creating instability.

To accomplish this for the direct region, first note that in the computational coordinates Equation (8) becomes

$$\left(\frac{dy}{dx}\right)_b = \frac{V_b}{U_b} = \frac{\sin\alpha + g_b\phi_{\eta_b}}{\cos\alpha + f_b\phi_{\xi_b}} \tag{16}$$

Here, Taylor series about the dummy point (i,j-1) (see Figure 2) can be used to express ϕ_{η_b} and ϕ_{ξ_b}. Thus,

$$\phi_{\eta_b} = \phi_{\eta_{i,j-1}} + (\eta_b - \eta_{j-1})\,\phi_{\eta\eta_{i,j-1}} + \ldots \tag{17}$$

$$\phi_{\xi_b} = \phi_{\xi_{i,j-1}} + (\eta_b - \eta_{j-1})\,\phi_{\xi\eta_{i,j-1}} + \ldots \tag{18}$$

When these are written in finite difference form using second order expressions for ϕ_ξ and ϕ_η and at least first order ones for $\phi_{\eta\eta}$ and $\phi_{\xi\eta}$, they become in the direct region (for the upper surface case)

$$\phi_{\eta_b} = \frac{-3\phi_{i,j-1} + 4\phi_{ij} - \phi_{ij+1}}{2\Delta_\eta} + (\eta_b - \eta_{j-1})\left(\frac{\phi_{i,j-1} - 2\phi_{ij} + \phi_{i,j+1}}{\Delta_\eta^2}\right) \tag{19a}$$

$$\phi_{\xi_b} = \frac{\phi_{i+1,j-1} - \phi_{i-1,j-1}}{2\Delta_\xi} + (\eta_b - \eta_{j-1})\left(\frac{\phi_{i+1,j} - \phi_{i+1,j-1} - \phi_{i-1,j} + \phi_{i-1,j-1}}{2\Delta\xi\Delta\eta}\right) \tag{19b}$$

These expressions can then be substituted into Equation (16) and the result solved for a sufficiently accurate $\phi_{i,j-1}$ that is in terms of the neighboring potentials, body slope, and body position.

In the inverse region the surface pressure boundary condition

$$\phi_{xb} = f_b\phi_{\xi b} = -\cos\alpha + \left\{\frac{1}{1 + \frac{V_b^2}{U_b^2}}\left\{1 - \frac{2}{(\gamma-1)M_\infty^2}\left\{\left[1 + \frac{\gamma M_\infty^2 C_{p_b}}{2}\right]^{\frac{\gamma-1}{\gamma}} - 1\right\}\right\}\right\}^{1/2} \tag{20}$$

must be applied at the location given for the surface by the previous relaxation sweep or last surface update. Thus, to start the inverse calculation an

initial profile is needed. While this profile should be reasonable and compatible with the shape selected for the nose region, it is not critical and the final airfoil may be quite different from the initial profile.

As in the direct region, the Taylor series expression for ϕ_{ξ_b}, Equation (18), is used in Equation (20); but in the inverse case considerable care must be used in selecting the finite difference forms for $\phi_{\xi i,j-1}$ and $\phi_{\xi\eta i,j-1}$. For example, since the resultant expression is to be solved for $\phi_{i,j-1}$, one possibility is to use $C_{p_{bi-1}}$ and central differences about (i-1,j-1). While numerically stable, this approach has two disadvantages. First, since the dominant term in the expansion is ϕ_ξ, central differencing causes $\phi_{i,j-1}$ to depend mostly upon $\phi_{i-2,j-1}$. Second, the pressure determining $\phi_{i,j-1}$ is $C_{p_{bi-1}}$ and not $C_{p_{bi}}$. Consequently, adjacent boundary points are uncoupled, and the boundary values usually have an undesirable oscillatory behavior. This can be mitigated slightly by using $C_{p_{bi-\frac{1}{2}}}$ and centering about $(i-\frac{1}{2},j-1)$, but the results are still frequently oscillatory.

In order to eliminate this oscillatory behavior, several other possible approaches were investigated. Among those found to be inaccurate and/or unstable were first order forward schemes using $C_{p_{bi-1}}$, first order backward formulas using $C_{p_{bi}}$, and schemes centered about (i,j-1) and using C_{p_i}. The latter failure was expected since its algebraic form emphasizes ϕ_η instead of ϕ_ξ. Finally, it was determined that a scheme based on (i,j-1) and that uses $C_{p_{bi}}$, second order backward differences in ξ on both ϕ_ξ and $\phi_{\xi\eta}$ and first order on η in $\phi_{\xi\eta}$ frequently worked very well.

However, the best form to use for $\phi_{\xi b}$ in Equation (20) is (for the upper surface)

$$\phi_{\xi_b} = \frac{3\phi_{i,j-1} - 4\phi_{i-1,j-1} + \phi_{i-2,j-1}}{2\Delta\xi} + (\eta_b - \eta_{j-1}) \left(\frac{\phi_{i+1,j} - \phi_{i+1,j-1} - \phi_{i-1,j} + \phi_{i-1,j-1}}{2\Delta\xi\Delta\eta}\right) \tag{21}$$

where the pressure coefficient is $C_{p_{bi}}$. This form does not introduce any numerical instabilities, builds into $\phi_{i,j-1}$ the upstream history of the airfoil, and uses $C_{p_{bi}}$. It leads to smooth boundary values and airfoil shapes with no apparent oscillations.

When Equation (21) is substituted into Equation (20) and the result solved for $\phi_{i,j-1}$, the final expression involves the square of the airfoil slope, V_b^2/U_b^2. Technically, this makes the equation nonlinear. However, since the surface slope is usually small in the inverse region, it has been found to be sufficiently accurate to hold $(V/U)_b$ constant at the value obtained for the last airfoil surface update.

For those situations where the flow at point (i,j) is supersonic, the rotated finite difference scheme may require a $\phi_{i,j-2}$ value as well as $\phi_{i,j-1}$. Thus, in all cases a value of $\phi_{i,j-2}$ is determined by extrapolation as

$$\phi_{i,j-2} = -\phi_{ij} + 2\phi_{i,j-1} \tag{22}$$

The above procedures for determining the values of the dummy mesh points inside the boundary is performed twice for the relaxation procedure of column i. First, either Eq. (16) or (20) are used with ϕ values obtained from the previous relaxation sweep in order to obtain old values for the dummy points $\phi_{i,j-1}$ and $\phi_{i,j-2}$. Then, after the column i has been relaxed, they are used again with as many current values of ϕ as possible to obtain new values $\phi^+_{i,j-1}$ and $\phi^+_{i,j-2}$. In this manner, the dummy mesh points will have both old and new values just like regular mesh points, and they can be used directly in the finite difference formulas without special treatment.

A similar procedure is used to satisfy the boundary conditions on the lower surface of the airfoil.

Now in the inverse case the airfoil shape must also be computed. In other words, for a given ϕ solution the differential equation given by Equation (16) must be solved for the surface ordinates, y, as a function of x, with the initial conditions given by the surface slope and ordinate at the interface between the direct and inverse regions. In the present problem the location of the interface and the values of the initial conditions are known because the nose region is solved directly. If the problem were treated completely inversely, the shape would depend upon the unknown value for ϕ at the leading edge.

An easy method for solving Equation (16) is to use the Euler-Cauchy (or Runge-Kutta of order two) method, either directly or with iteration, since it only requires information at i and i+1. This approach was tried, but it was found to be insufficiently accurate. Consequently, the Runge-Kutta method of

order four has been used; and while it requires for each step information at i, i+½, and i+1, the improvement in accuracy is worth the added complexity.

In the process of solving Equation (16) ϕ_{η_b} and ϕ_{ξ_b} must be evaluated by finite differences. While Equation (19a) is the obvious choice for ϕ_{η_b}, either Equation (19b) or (21) could be used for ϕ_{ξ_b}. Both have been used and both work well, but experience indicates that more accurate airfoil shape results are obtained using the central difference scheme, Equation (19b).

Finally, notice that in integrating Equation (16) the most difficult region from an accuracy standpoint is near the leading edge where the surface slopes are very large. In the present approach this difficulty is essentially eliminated since the nose shape is prescribed and the nose region is solved directly.

NUMERICAL STUDIES

Self Consistency

The present numerical method is capable of being used either directly or inversely. Thus, when pressure results from a direct calculation are used as an input for an inverse calculation, the original airfoil shape should be recovered. However, as shown by References (4-6), this task can be difficult; the key to success is numerical consistency between the direct and inverse computations. Hence, this type of test is a check on not only the validity of the inverse approach, but also on the consistency of the difference schemes. Several such tests have been conducted and some typical results are shown on Figures 3 and 4. Since the boundary condition in the inverse case is computed using Equation (20) combined with the backward difference formula, Eq. (21), the input C_p used in these tests (obtained from a direct calculation) was computed using Equation (21) for the ϕ_{ξ_b} term. In this manner, algebraic consistency between the two calculations is preserved.

Figure 3 compares the actual surface slopes with those computed by the inverse technique for a nonlifting NACA 0012 at slightly supercritical conditions. In this case, the inverse design region extended from 6% chord to the trailing edge. As can be seen the slopes, and consequently the shape, are returned exactly.

A more severe test of self-consistency is a supercritical lifting case, and the results of such a test are presented on Figure 4. Here a strong shock, having a local upstream Mach number of about 1.30, exists on the upper surface of the NACA 0012 airfoil. Notice that the agreement between the direct and inverse lift coefficients and between the actual and computed slopes is excellent, and that the differences between the upper and lower surface values are too small to be detected on the plot. For this case the computed surface ordinates are everywhere within 0.33% $(T/C)_{max}$ of the actual NACA 0012 ordinates, and no problems exist near the shock or the trailing edge.

Based upon these tests and results, it is believed that the present inverse design scheme and program is self-consistent and reasonably accurate.

Size of Inverse Region

The present design approach is general in that the interface between the direct and inverse regions can be located anywhere between the leading and trailing edges. However, the nose region is very hard to compute accurately in the inverse mode if the surface slopes are steep; and the question arises--How close to the leading edge can the inverse region start? To answer this question a series of inverse calculations were performed for a six percent biconvex airfoil at M_∞ of 0.9 and one degree angle of attack. The input C_p distribution, which contained shocks on both the upper and lower surfaces, was obtained from a direct computation, and in each of the tests the inverse zone was started at a different point. The inverse results were then compared with the actual surface slopes, given for the upper surface by the straight line $y_u' = -0.24(x/c) + .12$.

In making these comparisons it should be noted that the inverse boundary condition at point i, see Equations (20-21), uses information at points i, i-1, and i-2. Thus, if the inverse region starts at the third column from the leading edge, the inverse boundary condition uses only information aft of the leading edge. However, if the inverse region starts nearer the leading edge, information from in front of the airfoil will be used in the inverse boundary conditions, which may not be bad since the flow in front is subsonic and fully aware that there is an airfoil disturbing the flow.

The results of these tests are shown on Figure 5. The slopes computed by starting the inverse region at the third column from the leading edge are accurate, but those starting at the second are slightly in error on the slope and consequently also the shape. Finally, the slopes based upon the inverse region starting at the first column aft of the leading edge are in serious error. This trend has been verified by other tests with other airfoils. Consequently, it has been concluded that the inverse region should start no sooner than the third column from the leading edge, which is usually at about 5-10% chord. Hence, all the design results presented in this report have been computed with the inverse region starting no earlier than the third column aft of the leading edge.

Sensitivity to Errors in Cp

Since the pressure distribution is the primary input for the inverse mode, an important question is--How sensitive is the shape of the designed airfoil to errors in the input Cp distribution? This problem has been numerically investigated, and it has been found that a 0.5% change in all the C_p input values ($\Delta C_p \approx 0.003$) leads to a 0.5% $(T/C)_{max}$ change in the final airfoil ordinates. This increment appears small ($\Delta(y/c) \approx 0.0006$), but it can be quite significant in the vicinity of the trailing edge where ordinates tend to be small. While this result is not at all unexpected, it does mean that care should be exercised when using the inverse design program to insure the accuracy of the input C_p distribution.

COMPUTATIONAL PROCEDURE

In designing an airfoil shape using the inverse scheme, the same basic numerical relaxation technique as described in Reference (12) is used. To start the problem an initial airfoil shape must be assumed, but this choice is not critical and the final airfoil shape may be considerably different. Next, since experience has indicated that the inverse scheme works best if the perturbation potentials have reasonable starting values, fifty relaxation cycles are performed in the direct mode for the initial airfoil shape on a very coarse grid. Then, the grid spacing is halved and the inverse procedure is initiated using the input pressure distribution as the boundary condition in the inverse region.

An important consideration in the inverse calculations is the frequency of computing or updating the new airfoil shape. Since in the early relaxation cycles the pressure boundary condition may cause very large perturbations from the initial shape, it has been found best not to start the update procedure until after the first fifty iterative cycles on the second grid, which are all in the inverse mode. After that, updating can occur after each relaxation sweep, if desired, or at some specified interval, or after complete convergence has been achieved. The last is essentially the procedure used by Tranen.[7] Since each update computation requires a finite amount of computer time, it would be inefficient to calculate a new airfoil shape after each relaxation cycle. On the other hand, tests with the present scheme have indicated that updating only after convergence has been achieved usually yields airfoil shapes not completely compatible with the desired pressure distribution. It appears that the optimum procedure is to perform the airfoil shape update calculation after every ten relaxation cycles. More frequent updating does not improve the accuracy of the final shape and only wastes computer time, while less frequent use sometimes leads to small errors in the final shape. After convergence on the second grid, the spacing is halved at least once more and the entire procedure repeated.

Another important consideration in the inverse approach is the determination of convergence. In direct calculations, it is usually sufficient to monitor both the maximum perturbation potential change between relaxation cycles and the number of relaxation cycles. The calculation is stopped when either the maximum perturbation potential change is less than some specified value or the number of cycles exceeds a given number. However, in the inverse problem, another important criteria is the maximum change that occurs between update calculations in the surface ordinates of the airfoil being designed. It has been found that this value should also be monitored, and the computations continued until it is consistently less than some specified value (say $\Delta y/c < 0.0001$). Frequently, satisfaction of this criterion yields a maximum perturbation potential change smaller than would be required for a direct calculation.

All of the inverse results presented in this report have been obtained with this procedure and have used at least two grid halvings. Usually, the final grid contained 49 x 49 points, which yields 66 pressure points on the airfoil

surfaces. Typical computation times were six minutes on a CDC 6600 (including Varian plots) or about twenty minutes on an IBM 360/65.

APPLICATION AND TYPICAL RESULTS

When designing an airfoil to satisfy a specified pressure distribution, the final shape must have certain reasonable characteristics. Obviously, the upper and lower surface must not "criss-cross" near the trailing edge; and since the inverse approach yields the location of the boundary layer displacement surfaces, the trailing edge should have a finite thickness. Since the displacement thickness near the trailing edge is frequently on the order of 0.4% of the chord, the computed trailing edge thickness should be on the order of 1.0% or more. Unfortunately, it is not at all obvious how the input pressure distribution should be modified to achieve such characteristics if they do not result. Besides, such a modification would change one of the desired design parameters, namely, the pressure distribution.

With the present scheme, however, the pressure distribution can be kept the same, and the nose shape can be used by the designer to control the degree of tail closure. The procedure is demonstrated on Figure 6, which shows three airfoils, each designed with the same C_p distribution from 7% chord to the trailing edge. The input pressure distribution, which is shown as the solid line on Figure 7, is supposed to be "shockless" and contains the lower surface bucket typical of aft-cambered airfoils.

Airfoil No. 4 has an NACA 0012 nose shape; but, as can be seen on Figure 6, the resultant design has too thick a trailing edge. Consequently, a Korn-like nonsymmetrical nose shape (see Table I) having a smaller leading-edge radius was used. The resultant design, termed Airfoil No. 5 on Figure 6, is about two percent thinner and has a very reasonable trailing edge shape. Finally, for Airfoil No. 6, the lower surface nose region ordinates were raised by 0.1% of the chord; and this change led to a slightly thinner airfoil with an even thinner trailing edge.

Figure 8 shows another case in which the nose shape was used to control the trailing edge characteristics. The pressure distribution for these airfoils, which is the solid curve on Figure 9, was selected to have the same basic lift coefficient and lower surface pressure distribution as an NACA 0012

at the same flight conditions, but without the strong upper surface shock wave. In each case, the nose shapes and initial starting profiles were those associated with NACA OOXX airfoils. For the NACA 0010 nose shape, Airfoil No. 100, the upper and lower surfaces of the designed airfoil criss-crossed; but, as can be seen on Figure 8 for Airfoils 110 and 115, as the leading edge radius was increased, the maximum and trailing edge thicknesses also increased proportionately. In each case, the moment coefficient was low compared to similar aft-cambered airfoils, and the maximum upper surface ordinate was near the mid-chord.

Based upon the results shown in Figures 6 and 8, it is believed that the nose shape can be used to control the trailing edge shape and that any desired thickness of the trailing edge displacement surfaces can be achieved by the designer by adjusting the nose shape. As indicated previously, this adjustment does not require changing the desired inverse C_p distribution.

Now a severe test for a design program is whether or not an analysis or direct solution of the designed airfoil returns the design or inverse C_p distribution. Figure 7 compares the inverse C_p used to design Airfoil No. 5 with that obtained from a direct solution (airfoil given) using the ordinates for No. 5, and Figure 9 makes a similar comparison for Airfoil No. 115. In these comparisons the input C_p is used with ϕ_{ξ_b} computed via backward differences (Equation (21)), while the direct C_p results are based upon more usual central differences. As a result, perfect agreement should not be expected. Nevertheless, the agreement in both cases is excellent. On Figure 7, the lower surface result agrees perfectly; and the direct solution for the upper surface only disagrees slightly near 70% chord, exhibiting a weak shock (local Mach number of 1.07) at 84% chord. This appearance of a weak shock and the consequent variation in lift coefficient of about two percent frequently appears when aft-cambered airfoils that are designed to be shockless are analyzed directly.[2] The comparisons for Airfoil No. 115 on Figure 9 show even better agreement and tend to verify the validity and accuracy of the present inverse design program.

A final case is shown on Figure 10. An arbitrary pressure distribution (dashed line) having an upper surface Mach number plateau around 1.2 followed by a large jump to subsonic flow at 76% chord was selected for the inverse

input. No attempt was made to match the shock jump conditions at the discontinuity. On the lower surface, the C_p was chosen to maintain subsonic flow; and a pressure bucket selected according to the Stratford separation criteria[14] was included to enhance lift. As indicated, the design program uses for ϕ_{ξ_b} a backward difference scheme, Eq. (21) with the C_p boundary condition, Eq. (20); and, thus, in regions of large gradients the output pressure distribution, which is computed using a central scheme for ϕ_{ξ_b} and should be more accurate, will be different.

Now in the course of the inverse solution, the trailing edge displacement surfaces that satisfied the input C_p distribution were not parallel; and, thus, the inviscid solution required a rear stagnation point behavior. The actual inverse pressure distribution, which was computed by central differences and is indicated on Figure 10 by the solid line, shows this behavior. (Of course, if the converged solution was used to compute C_p using backward difference for ϕ_{ξ_b} as in Eq. (21), the prescribed "inverse input" distribution would be obtained.) In addition, notice that the upper surface discontinuity has been smoothed. Examination of the flowfield results shows a smooth supersonic bubble on the upper surface and indicates that the decelleration, while rapid, is not due to a shock wave of any significant strength. Also shown on Figure 10 are the results of a direct solution for the designed airfoil, which exhibit excellent agreement with the actual inverse pressure coefficient distribution. Finally, the airfoil shown is the shape obtained after the boundary layer displacement thickness, calculated by the method of Nash-McDonald[2] for a Reynolds number of twenty million, has been subtracted.

It is believed that the results of Figure 10 demonstrate that the present inverse technique and program can handle "arbitrary" pressure inputs. In addition, it will yield results consistent with analysis technique.

CONCLUDING REMARKS

An inverse technique suitable for designing two-dimensional transonic airfoils having a specified pressure distribution has been developed. This method utilizes the full inviscid potential flow equation and exact boundary conditions and solves them via numerical relaxation. A rotated finite difference scheme is employed in order to obtain the correct domain of dependence

in supersonic regions, and Jameson's time-like damping is included to insure numerical stability. Further, grid halving is used to achieve computational efficiency.

A logical method for controlling trailing edge closure has been developed. In addition, it has been demonstrated that it is not necessary to match the computational grid to the airfoil surface and that very accurate, numerically consistent, and physically correct results can be obtained in a Cartesian grid system. The technique has been successfully used to design aft-cambered and other airfoils specifically for transonic flight.

Texas A&M University
Aerospace Engineering Department
College Station, Texas
14 December 1974

REFERENCES

1. Nieuwland, G.Y.: Transonic Potential Flow Around a Family of Quasi-Elliptical Aerofoil Sections. NLR-TR-T. 172, National Lucht-en Ruimtevaart Laboratorium, Amsterdam, 1967.
2. Bauer, F.; Garabedian, P.; and Korn, D.: A Theory of Supercritical Wing Sections, with Computer Programs and Examples. Springer-Verlag, 1972.
3. Hicks, R.M.; Murman, E.M.; and Vanderplaats, G.N.: An Assesment of Airfoil Design by Numerical Optimization. NASA TM X-3092, July 1974.
4. Erdos, J; Baronti, P.; and Elzweig, S.: Transonic Viscous Flow Around Lifting Two-Dimensional Airfoils. AIAA Paper 72-678, June 1972.
5. Steger, J.L.; and Klineberg, J.M.: A Finite-Difference Method for Transonic Airfoil Design, AIAA J., Vol. 11, No. 5, May 1973, pp. 628-635.
6. Carlson, L.A.: Inverse Transonic Flow Calculations Using Experimental Pressure Distributions. AIAA J., Vol. 12, No. 4, April 1974, pp. 571-572.
7. Tranen, T.L.: A Rapid Computer Aided Transonic Airfoil Design Method. AIAA Paper No. 74-501, June 1974.
8. Whitcomb, R.T.: Review of NASA Supercritical Airfoils. Proc. of the IXth ICAS Congress, Haifa, Israel, Paper No. 74-10, August 1974.
9. Garabedian, P.R.; and Korn, D.G.: Analysis of Transonic Airfoils. Comm. on Pure and Applied Math., Vol. 24, 1971, pp. 841-851.
10. South, Jr., J.C.; and Jameson, A.: Relaxation Solutions for Inviscid Axisymmetric Transonic Flow Over Blunt or Pointed Bodies. Proc. AIAA Computational Fluid Dynamics Conference., Palm Springs, Calif., July 1973, pp. 8-17.
11. Jameson, A.: Iterative Solution of Transonic Flows Over Airfoils and Wings, Including Flows at Mach 1: Comm. on Pure and Applied Math., Vol. 27, 1974, pp. 283-309.
12. Carlson, L.A.: Transonic Airfoil Flowfield Analysis Using Cartesian Coordinates. NASA CR-2577, August 1975.
13. Ludford, G.S.S.: The Behavior at Infinity of the Potential Function of a Two Dimensional Subsonic Compressible Flow. J. Math. Phys., Vol. 30, No. 3, Oct. 1951, pp. 117-130.

14. Stratford, B.S.: The Prediction of Separation of the Turbulent Boundary Layer. J. Fluid Mech., Vol. 5, 1959, pp. 1-16.

	Airfoil No. 4		Airfoil No. 5		Airfoil No. 6	
$\frac{x}{c}$	$\frac{y_u}{c}$	$\frac{y}{c}$	$\frac{y_u}{c}$	$\frac{y}{c}$	$\frac{y_u}{c}$	$\frac{y}{c}$
0.0000	0.0	0.0	0.0	0.0	0.0	0.0
0.0100	0.0170	-0.0170	0.0161	-0.0159	0.0161	-0.0149
0.0248	0.0260	-0.0260	0.0260	-0.0223	0.0260	-0.0213
0.0396	0.0321	-0.0321	0.0322	-0.0263	0.0322	-0.0253
0.0544	0.0368	-0.0368	0.0365	-0.0293	0.0365	-0.0283

Table I--Nose Shape Ordinates

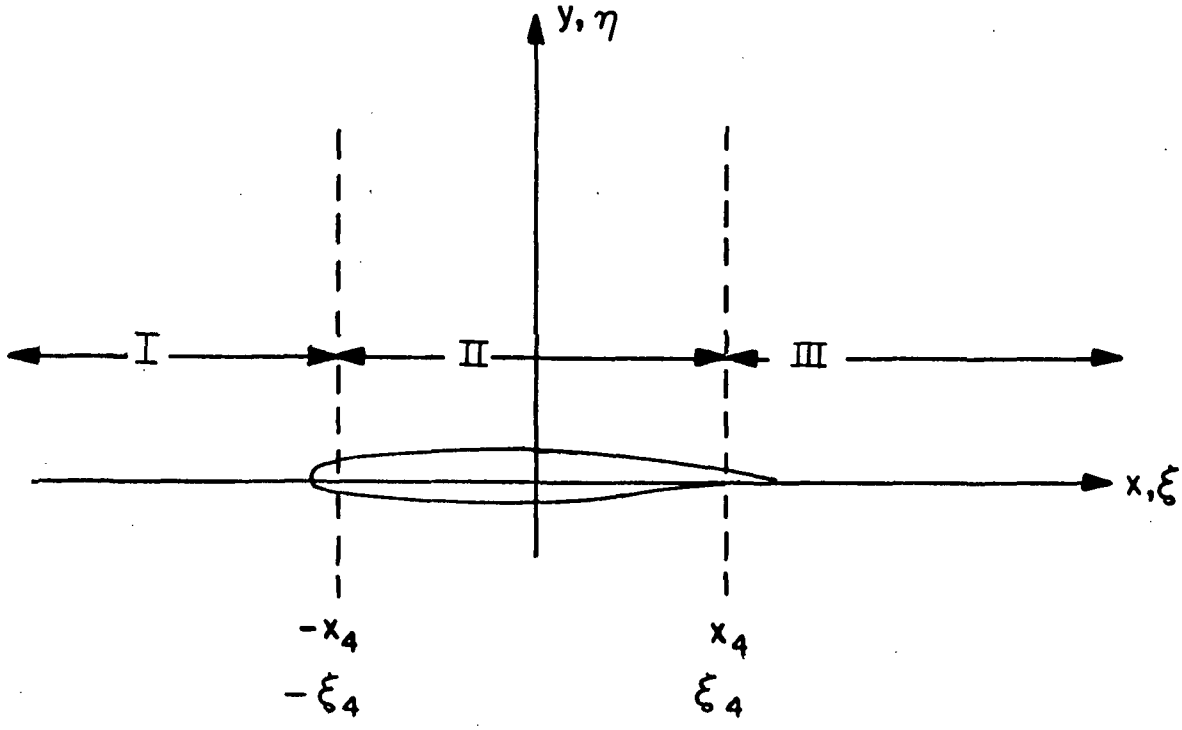

Figure 1--Flowfield Subdivision for Coordinate Stretching

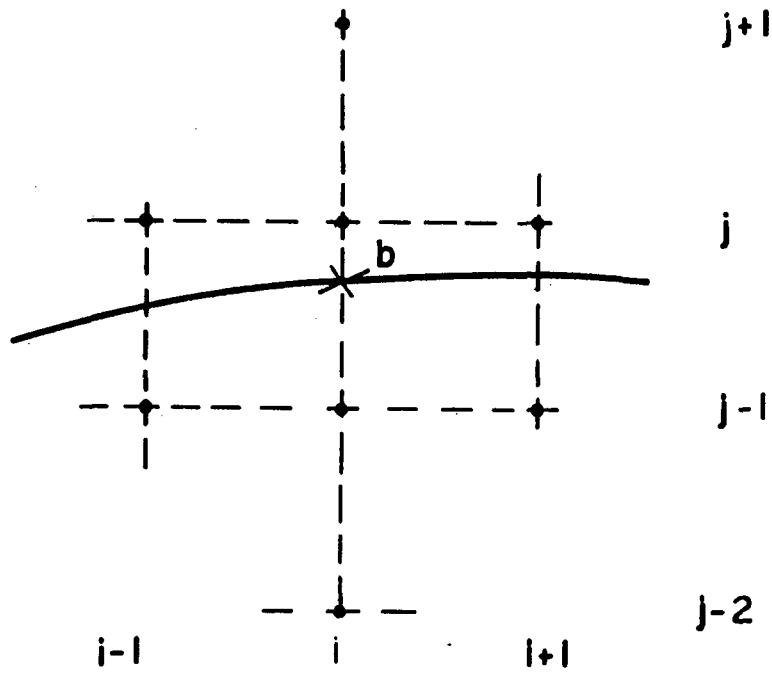

Figure 2--Relationship Between Airfoil and Grid (Upper Surface)

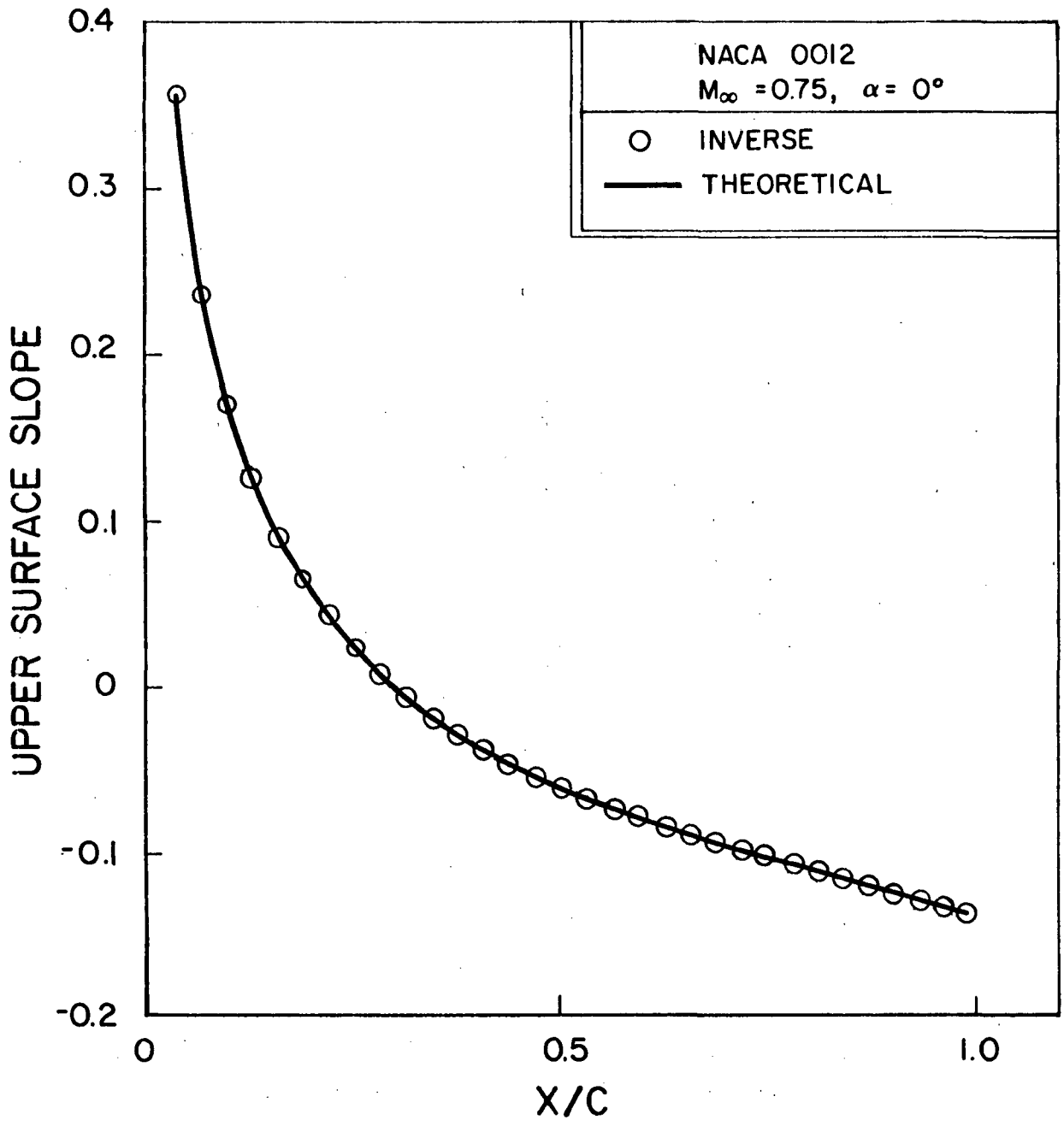

Figure 3--Comparison of Actual Airfoil Slopes with Those Computed by Design Program (Nonlifting Case)

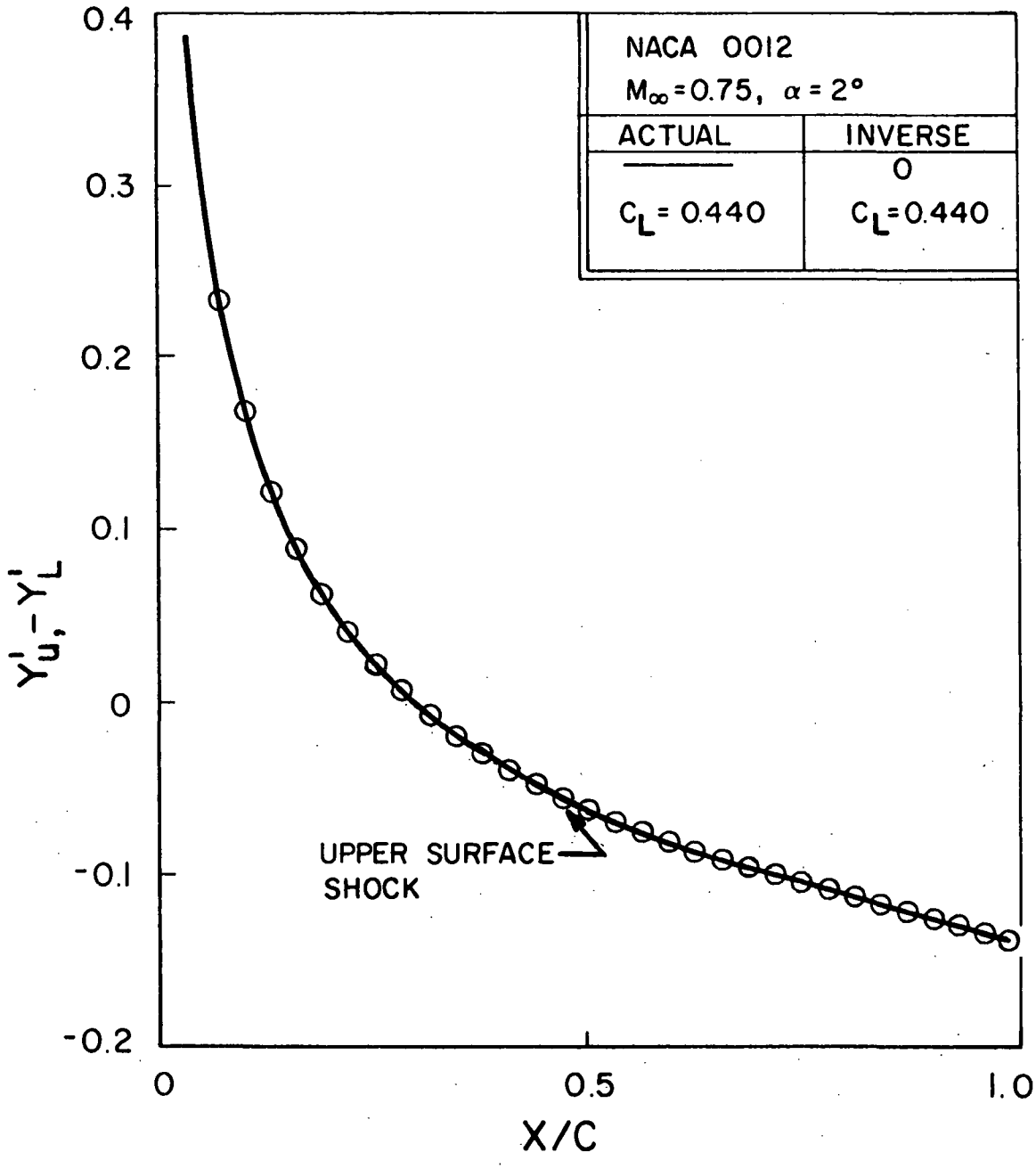

Figure 4--Comparison of Actual Airfoil Slopes with Those Computed by Design Program (Lifting Case)

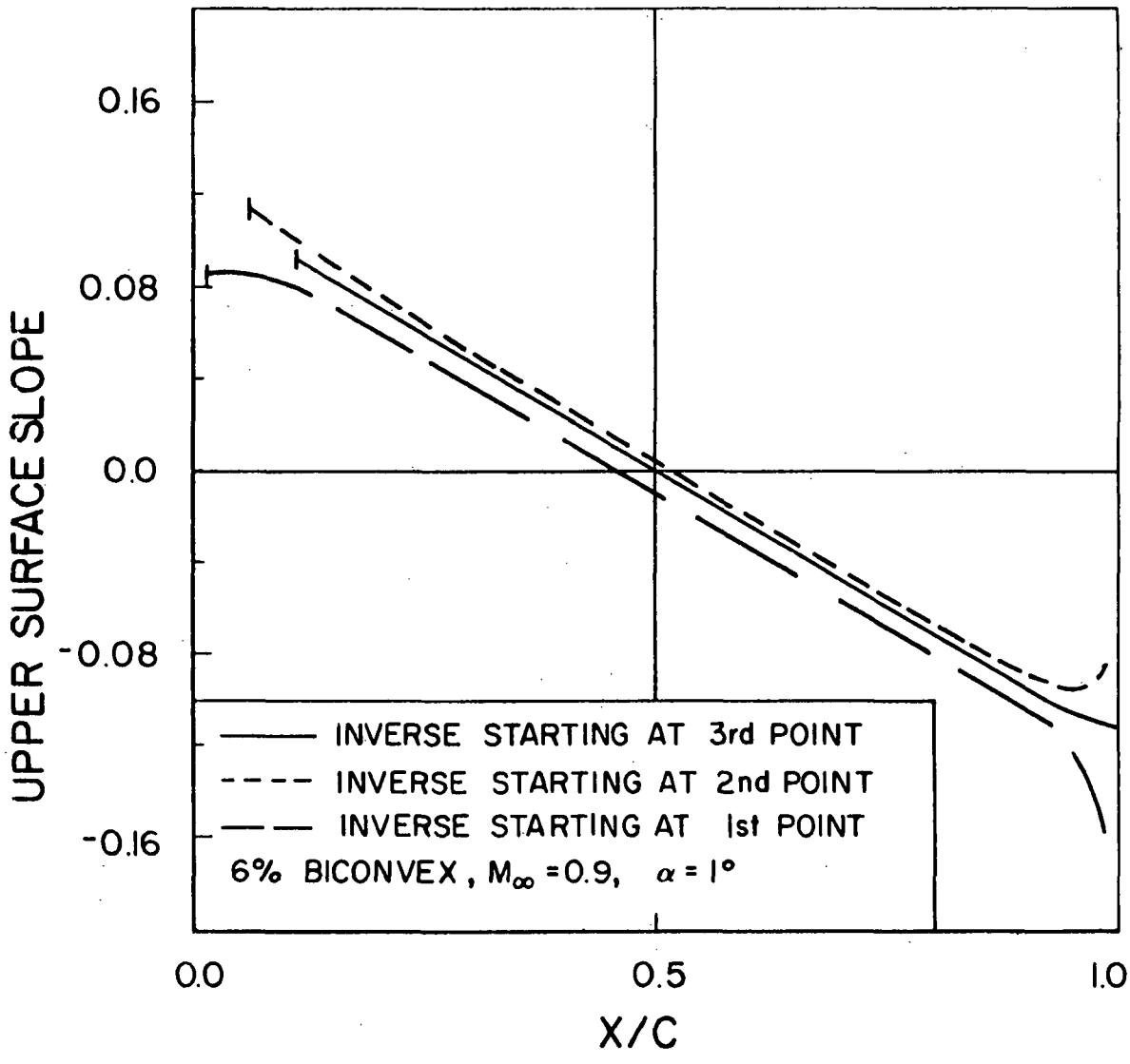

Figure 5--The Effect of the Size of the Initial Direct Region

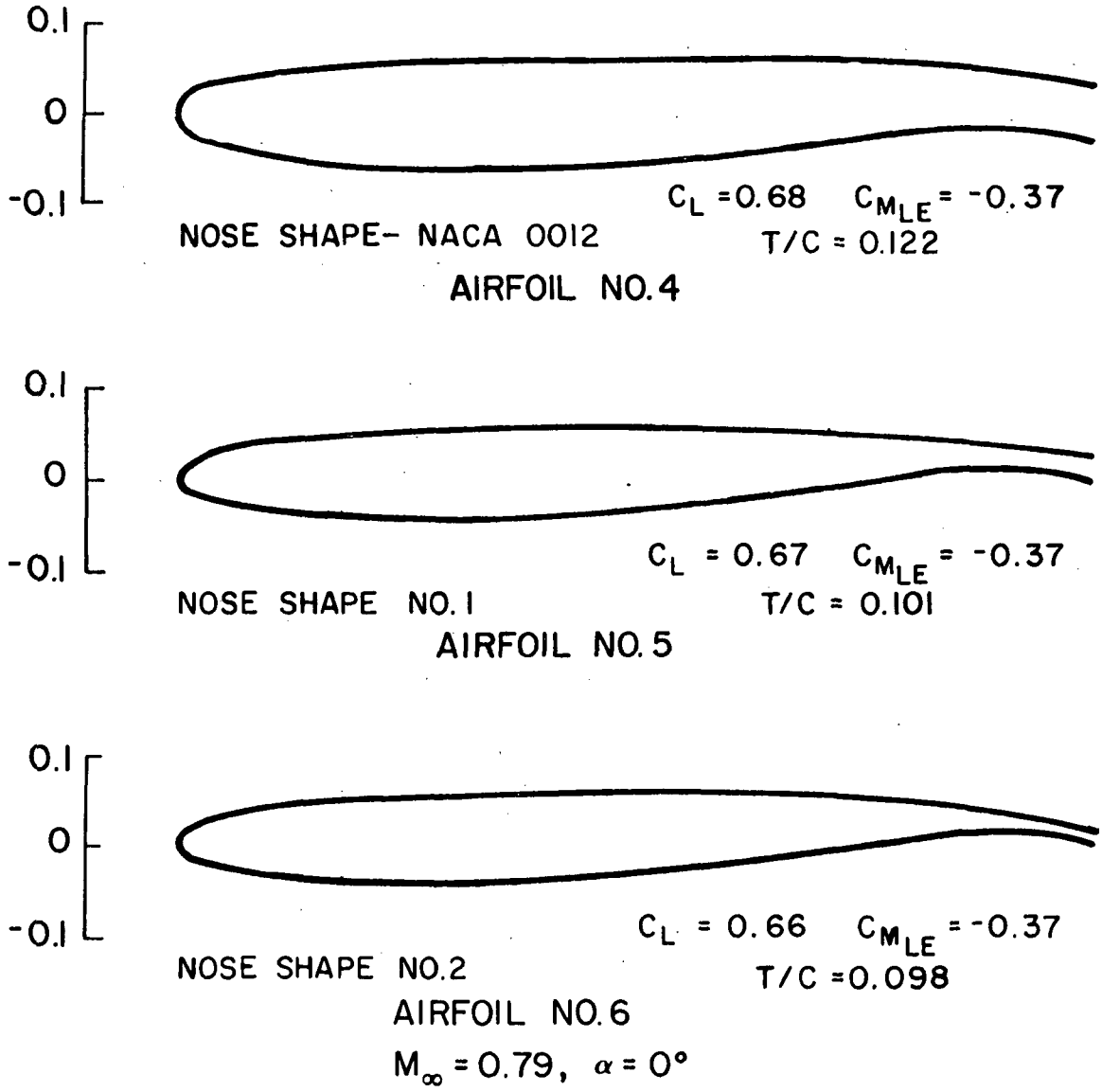

Figure 6--The Use of Nose-Shape to Control Trailing Edge Closure, Example 1

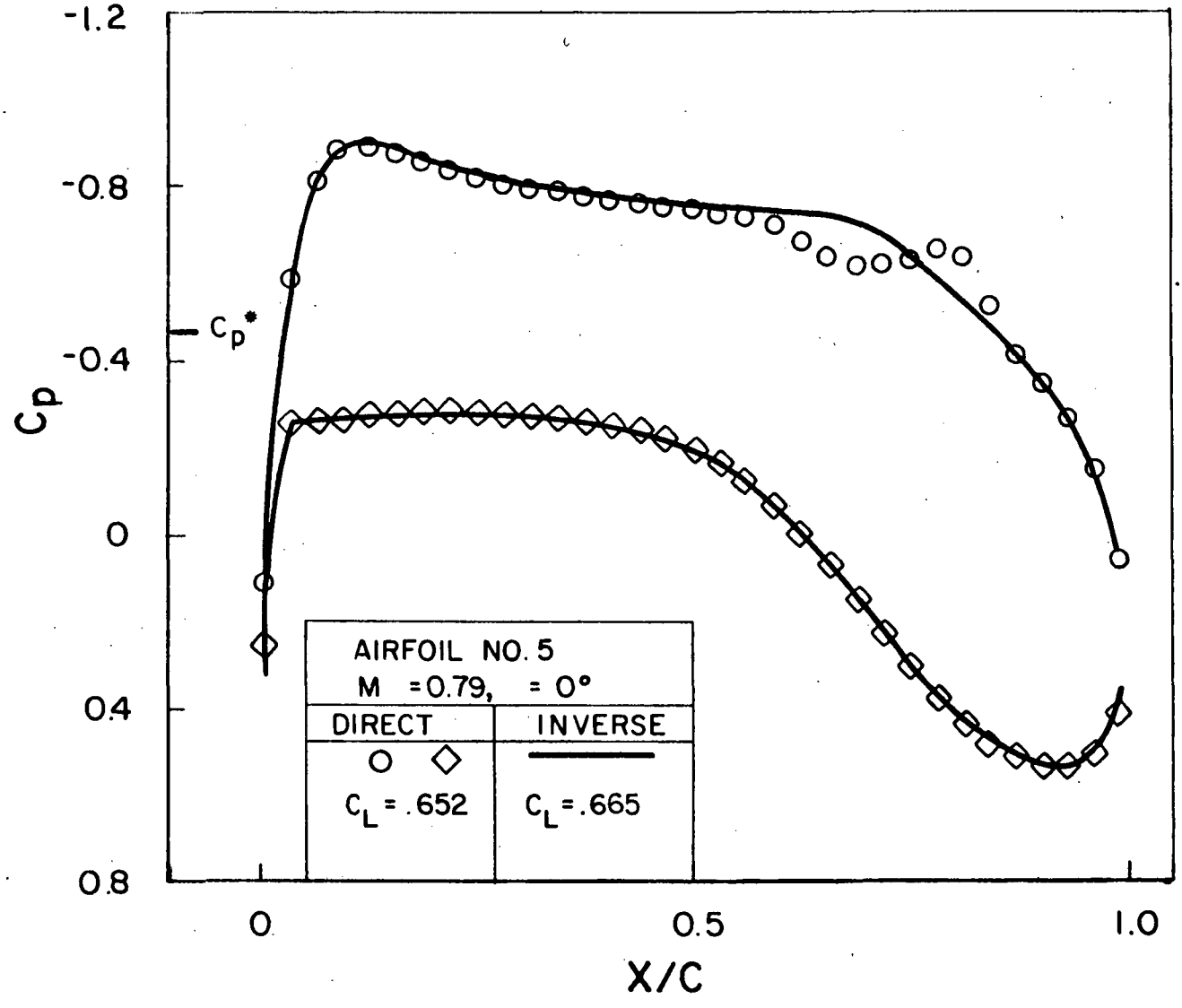

Figure 7--Comparison of Inverse C_p Distribution with that Obtained by Analysis of Designed Airfoil, Example 1

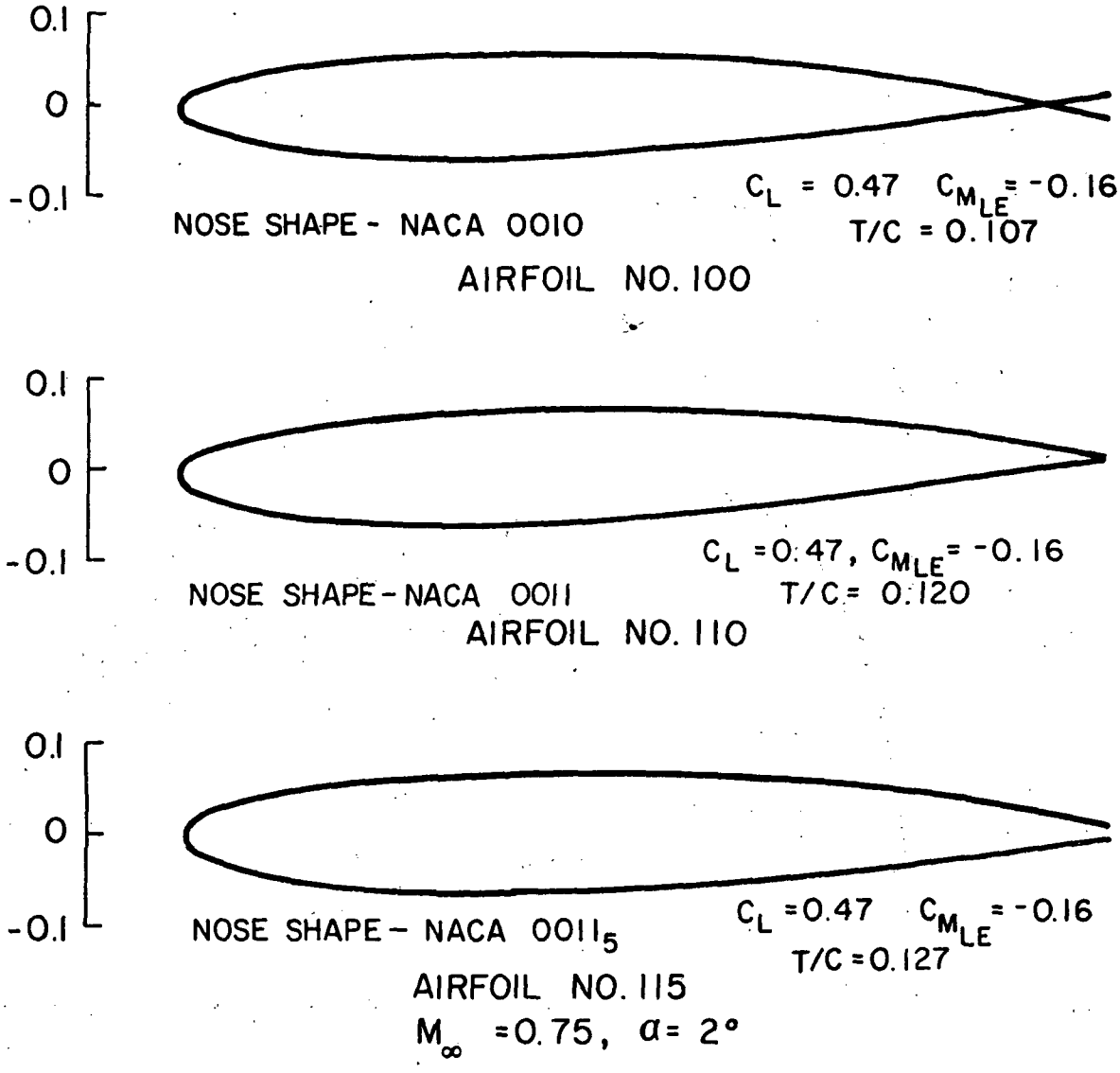

Figure 8--The Use of Nose Shape to Control Trailing Edge Closure, Example 2

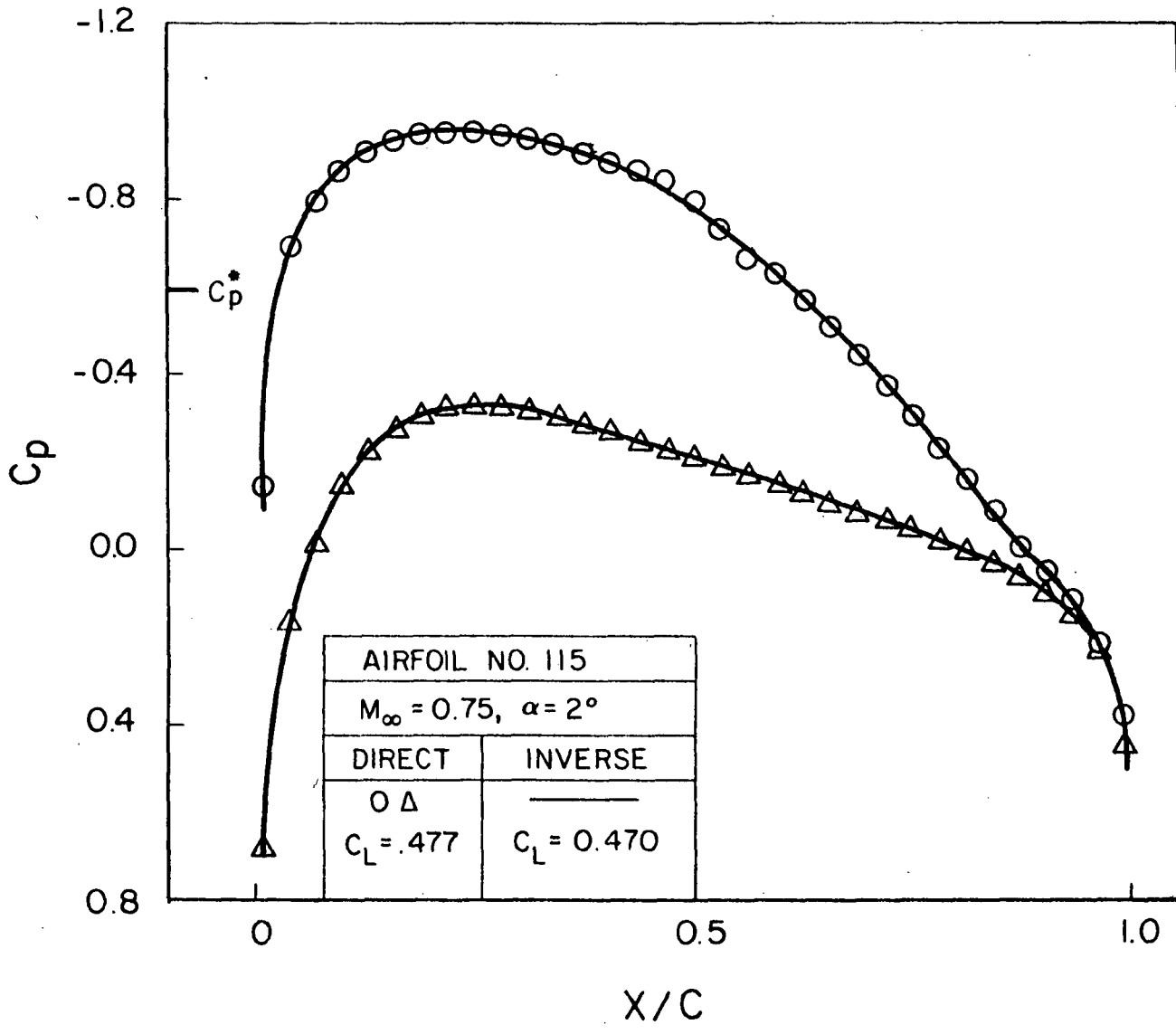

Figure 9--Comparision of Inverse C_p Distribution with that Obtained by Analysis of Designed Airfoil, Example 2

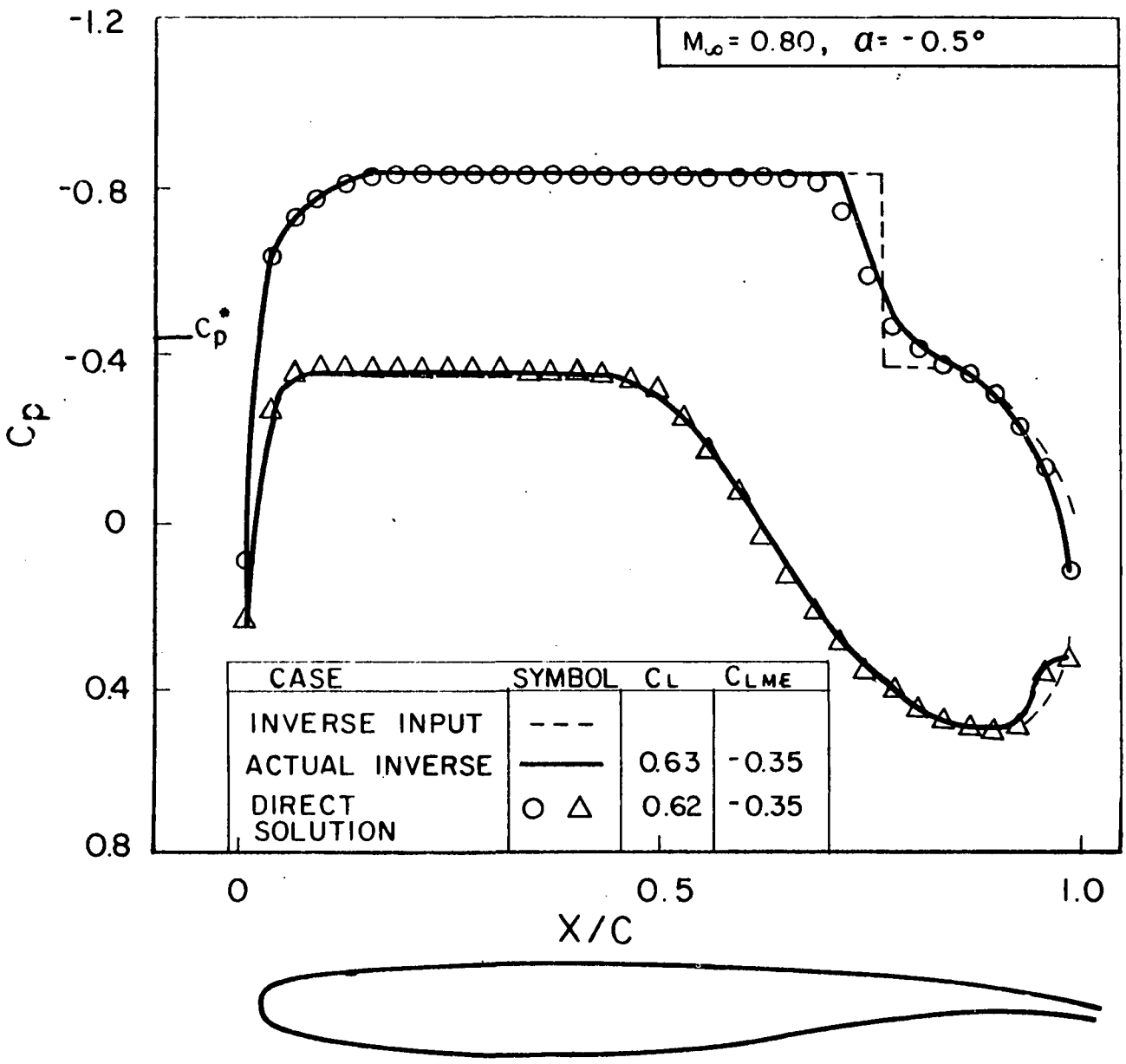

Figure 10--Comparison of C_p Distributions

NATIONAL AERONAUTICS AND SPACE ADMINISTRATION
WASHINGTON, D.C. 20546

OFFICIAL BUSINESS
PENALTY FOR PRIVATE USE $300

SPECIAL FOURTH-CLASS RATE
BOOK

POSTAGE AND FEES PAID
NATIONAL AERONAUTICS AND
SPACE ADMINISTRATION
451

U.S.MAIL

POSTMASTER: If Undeliverable (Section 158 Postal Manual) Do Not Return

"The aeronautical and space activities of the United States shall be conducted so as to contribute . . . to the expansion of human knowledge of phenomena in the atmosphere and space. The Administration shall provide for the widest practicable and appropriate dissemination of information concerning its activities and the results thereof."

—NATIONAL AERONAUTICS AND SPACE ACT OF 1958

NASA SCIENTIFIC AND TECHNICAL PUBLICATIONS

TECHNICAL REPORTS: Scientific and technical information considered important, complete, and a lasting contribution to existing knowledge.

TECHNICAL NOTES: Information less broad in scope but nevertheless of importance as a contribution to existing knowledge.

TECHNICAL MEMORANDUMS: Information receiving limited distribution because of preliminary data, security classification, or other reasons. Also includes conference proceedings with either limited or unlimited distribution.

CONTRACTOR REPORTS: Scientific and technical information generated under a NASA contract or grant and considered an important contribution to existing knowledge.

TECHNICAL TRANSLATIONS: Information published in a foreign language considered to merit NASA distribution in English.

SPECIAL PUBLICATIONS: Information derived from or of value to NASA activities. Publications include final reports of major projects, monographs, data compilations, handbooks, sourcebooks, and special bibliographies.

TECHNOLOGY UTILIZATION PUBLICATIONS: Information on technology used by NASA that may be of particular interest in commercial and other non-aerospace applications. Publications include Tech Briefs, Technology Utilization Reports and Technology Surveys.

Details on the availability of these publications may be obtained from:

SCIENTIFIC AND TECHNICAL INFORMATION OFFICE

NATIONAL AERONAUTICS AND SPACE ADMINISTRATION

Washington, D.C. 20546